Apolipoprotein A-I Directly Interacts with Amyloid Precursor Protein and Inhibits Aβ Aggregation and Toxicity†

Radosveta P. Koldamova, Iliya M. Lefterov, Martina I. Lefterova, and John S. Lazo*

Department of Pharmacology, University of Pittsburgh, School of Medicine, Pittsburgh, Pennsylvania 15261

Received September 18, 2000; Revised Manuscript Received January 26, 2001

ABSTRACT: Amyloid precursor protein (APP) is the source of the neurotoxic amyloid β (Aβ) peptide associated with Alzheimer's disease. Apolipoprotein A-I (apoA-I), a constituent of high-density lipoprotein complexes, was identified by a yeast two-hybrid system as a strong and specific binding partner of full-length APP (APPfl). This association between apoA-I and APPfl was localized to the extracellular domain of APP (APPextra). Furthermore, the interaction between apoA-I and APPfl was confirmed by coprecipitation using recombinant epitope-tagged APPextra and purified apoA-I. Several functional domains have been identified in APPextra, and we focused on a possible interaction between apoA-1 and the pathologically important Aβ peptide, because APPextra contains the nontransmembrane domain of Aβ. The binding between apoA-I and Aβ was saturable (K_d = 6 nM), specific, and reversible. APPextra also competed with apoA-I for binding to Aβ. Direct evidence for this interaction was obtained by the formation of an SDS-resistant Aβ−apoA-I complex in polyacrylamide gels. Competitive experiments with apolipoprotein E (isoforms E2 and E4) showed that apoA-I had a higher binding affinity for Aβ. We also found that apoA-I inhibited the β-sheet formation of Aβ with a mean inhibitory concentration close to that of α2-macroglobulin. Finally, we demonstrated that apoA-I attenuated Aβ-induced cytotoxicity. These results suggest apoA-I binds to at least one extracellular domain of APP and has a functional role in controlling Aβ aggregation and toxicity.

Alzheimer's disease (AD)[1] is a neurodegenerative disorder characterized by the presence of senile plaques (SP) in the brain and cerebral blood vessels, neurofibrillary tangles, and neuronal loss (*1*−*3*). SP are composed primarily of highly insoluble AD-specific aggregates of amyloid β (Aβ) peptide. Aβ is a 40−43 amino acid fragment of a larger, class I transmembrane protein named amyloid precursor protein (APP) (*4, 5*). The structure of APP resembles a cell surface receptor or growth factor, although few ligands that interact with its large ectodomain have been found (*6*). To generate Aβ, APP is cleaved by two proteases: a recently cloned β-secretase (an aspartyl protease called BACE1) and the more enigmatic γ-secretase (*7, 8*). Cleavage by α-secretase in the lumenal domain of APP precludes Aβ formation by producing p3 and soluble APPα (sAPPα) (*9, 10*). sAPPα has been shown to protect neurons against numerous detrimental stimuli like ischemia, glucose deprivation, and glutamate (*11, 12*). On the other hand, Aβ aggregation and amyloid fibril formation may initiate neurodegeneration, because neuronal loss in vivo is accompanied by deposition of Aβ fibrils in SP. Therefore, understanding the mechanism of Aβ fibril growth may help in the development of compounds that inhibit Aβ amyloidogenesis and consequently Aβ-induced toxicity.

While the events by which soluble nontoxic Aβ peptides are converted to amyloid fibrils in AD are unclear, Aβ nucleation is essential. This nucleation depends on protein concentration, pH, and the presence of ancillary binding molecules. For example, binding of Aβ to the membrane or proteoglycans can create a higher effective local concentration and increase the probability for aggregation. In contrast, proteins such as apolipoprotein E2 (apoE2), apolipoprotein E3 (apoE3), apolipoprotein J (apoJ), and α2-macroglobulin (α2M) have been shown to interact with Aβ and to inhibit its aggregation (*13*−*16*). The inheritance of the apoE4 allele of *APOE* is associated with an increased risk of late-onset sporadic and familial AD (*17*). ApoE4 was found to increase Aβ aggregation and Aβ-induced neurotoxicity in contrast to apoE2 and apoE3, but otherwise the physiological difference among the *APOE* isoforms has not been established (*18*). Brain apolipoproteins, like apoE, apoJ, and apoA-I, have previously been found in SP of AD patients, and Aβ has been shown to interact with apolipoproteins from cerebrospinal fluid (CSF) and plasma (*19*−*21*). ApoA-I and apoE are

† This work was supported by USPHS Grant CA43917, University of Pittsburgh Alzheimer's Disease Research Center Grant AG 05133, and the Fiske Drug Discovery Fund.

* To whom correspondence should be addressed at the Department of Pharmacology, University of Pittsburgh, School of Medicine, Pittsburgh, PA 15261. Tel.: 412-648-9319; Fax: 412-648-2229; E-mail: lazo@pitt.edu.

[1] Abbreviations: AD, Alzheimer's disease; α2M, α2-macroglobulin; Aβ, amyloid β; apoA-I, apolipoprotein A-I; apoE, apolipoprotein E; APP, amyloid precursor protein; APPcyto, cytoplasmic domain of APPfI; APPextra, extracellular domain of APP; APPfl, full-length amyloid precursor protein; β-gal, β-galactosidase; BD, binding domain of GAL4; BSA, bovine serum albumin; CSF, cerebrospinal fluid; CR, Congo red; ELISA, enzyme-linked immunosorbent assay; HDL, high-density lipoprotein(s); IC_{50}, half-maximal inhibition concentration; LAM, lamin; MTT, 3-[4,5-dimethylthiazol-2-yl]-2,5-diphenyltetrazolium bromide; mAb, monoclonal antibody; PBS, phosphate-buffered saline; sAPP, secreted soluble APP; sAPPα, sAPP resulting from α-secretase cleavage; SP, senile plaques; YTH, yeast two-hybrid system.

10.1021/bi002186k CCC: $20.00
Published on Web 02/27/2001

major apolipoproteins identified in CSF associated with high-density lipoproteins (HDL) (*22*), and, as constituents of HDL, they have an important role in controlling the lipid homeostasis in peripheral cells. Although the in vivo biological function of brain apolipoproteins is less clear, an involvement of them in transporting cholesterol to and out of neurons seems plausible. Considerable attention has been placed on understanding the role of apoE in AD and in brain lipid homeostasis, but other apolipoproteins, such as apoA-I, have largely been ignored, perhaps because there is no evidence for apoA-I synthesis in neuronal cells.

As a part of an ongoing effort to identify proteins that interact in vivo with APPfl and, therefore, might participate in the pathogenesis of AD, we screened a liver library using the yeast two-hybrid (YTH) system. Surprisingly, we found apoA-I was one of the proteins with a strong and specific interaction with APPfl. The interaction was restricted to the extracellular domain of APP (APPextra), which contains the entire region of sAPPα. We also found that apoA-I associated with Aβ in vitro and inhibited its β-sheet formation and Aβ-induced cytotoxicity.

MATERIALS AND METHODS

cDNA, Expression Vectors, and Site-Directed Mutagenesis. pCite4APP$_{695wt}$ was generated by PCR cloning as described (*23*). APP$_{695wt}$ was excised from pCite4APP$_{695wt}$ and cloned into *Nde*I−*Sal*I-digested pAS2-1 (Clontech, Palo Alto, CA), thus generating pAS2-1APP$_{695wt}$, which we used as a bait for YTH screening.

APPextra was generated using pCite4APP$_{695wt}$ as a template and the following primers: forward, 5′-GTGGAATC-CATATGCTGCCCGGTTT-3′; reverse, 5′-GCGCGTCGAC*T-TA*GTTTGAACCCACATCTTCT-3′ (*Nde*I and *Sal*I recognition sites are underlined). A stop codon (shown in italics) was generated by mutating Lys28 within the Aβ sequence and was inserted before the *Sal*I recognition site. APPextra was excised by restriction enzyme digestion and ligated into *Nde*I−*Sal*I-linearized pAS2-1 or pET28 (Novagen, Madison, WI), thus generating pAS2-1 APPextra for YTH binding or pET28APPextra for prokaryotic expression and in vitro binding experiments.

Oligonucleotide-directed site-specific mutagenesis was performed using the QuickChange mutagenesis kit (Stratagene, San Diego, CA) for generation of the cytoplasmic tail of APPwt. Oligonucleotides complementary to the both strands of APPwt were synthesized to insert a *Nde*I recognition site before amino acid 724 (770 numbering): forward, 5′-CACCTTGGTGCATATGAAGAAGAAACAGT-3′; reverse, 5′-ACTGTTTCTTCTTCATATGCACCAAGGTG-3′. The template used for PCR was pCite4APP$_{695wt}$, and the procedure was performed as previously described (*23*). The mutated template was subjected sequentially to *Nde*I digestion and religation, thus generating pCite4APPcyto, which we used as a source to digest and transfer APPcyto into pAS2-1.

The in-frame position of all cDNA inserts was confirmed by dye terminator labeling and sequencing using an ABI Prism 377 DNA Sequencer (University of Pittsburgh Research Support Facility).

Yeast Two-Hybrid Screening. YTH screening and analysis were performed as previously described (*24*). Briefly, we used the Matchmaker2 protocol provided by Clontech with the Y190 yeast strain (MATa, ura3−52, his3−200, lys2−801, ade2−101, trp1−901, leu2−3,112, gal4, gal80, cyhr2, LYS2::GAL1UAS-HIS3TATA-HIS3,URA3::GAL1UAS-GAL1TATA-lacZ). Human liver cDNA library was purchased from Clontech and Y190 cotransformed with pVA3 and pTD, which served as positive controls (*24*). We confirmed the expression of the GAL4-APPfl and APPextra fusion proteins by Western immunoblotting with N-terminal anti-APP monoclonal antibody (mAb) (LN27, Zymed, South San Francisco, CA) and anti-BD mAb (Clontech) against the binding domain of GAL4. Qualitative and quantitative β-galactosidase assays were measured as previously described (*24*). To evaluate quantitatively β-galactosidase activity, we used an *o*-nitrophenyl-β-D-galactosidase colorimetric assay (Pierce, Rockford, IL) according to the manufacturer's instructions.

In Vitro Coprecipitations of His-APPextra and ApoA-I. The expression and purification of his-tagged APPextra (his-APPextra) were done as previously described for other his-tagged proteins (*25*). Human apoA-I (4 μg) (Sigma, St. Louis, MO) was incubated with increasing concentrations of his-APPextra in phosphate-buffered saline (PBS, pH 7.4) for 30 min at 4 °C. The protein mixtures were diluted 2-fold in PBS containing 1% Triton X-100 and incubated for 30 min with nickel−agarose resin (Qiagen, Valencia, CA). The resin was collected by centrifugation, washed 4−5 times with PBS/Triton X-100, and boiled in the presence of Laemmli sample buffer. The precipitated proteins were separated on 12% SDS−PAGE gels (Novex, Carlsbad, CA). Gels were transferred to Protran nitrocellulose membranes (Schleicher & Schuell, Dassel, Germany) and probed with anti-APP mAb LN27 antibody or anti-apoA-I mAb (Calbiochem, La Jolla, CA). The blots were probed with horseradish peroxidase-conjugated secondary antibodies (Jackson Immuno Research Laboratories, West Grove, PA) and developed with a Renaissance chemiluminescence kit from NEN (Boston, MA).

ApoA-I and Aβ Complex Formation and Detection. In vitro binding studies between apoA-I and Aβ(1−40) (Bachem, King of Prussia, PA) were done by incubating a mixture of 1 μg of apoA-I and 4 μg of Aβ(1−40) in PBS (pH 7.4) in a 30 μL volume at 37 °C for 18 h. Control reactions were incubated without apoA-I or Aβ(1−40). The reactions were stopped by addition of 2 × reducing Laemmli buffer (4% SDS, plus mercaptoethanol) and boiled for 5 min. The resultant complexes were separated on 10−20% Tricine gels (Novex), transferred to nitrocellulose membranes, and probed with anti-Aβ (anti-Aβ1−16, BioSource, Camarillo, CA) mAb and with anti-apoA-I mAb. The blots were probed with horseradish peroxidase-conjugated secondary antibodies visualized as described above.

Enzyme-Linked Immunosorbent Assay (ELISA). The interaction of apoA-I with Aβ(1−40) was studied by ELISA using synthetic Aβ(1−40) as previously described (*13*). Briefly, polystyrene microtiter plates (Costar, Greenwich, CT) were coated with Aβ(1−40) (400 ng in well) in 0.1 M $NaHCO_3$, pH 8.6, overnight at 4 °C. Previously it has been shown that under the same conditions 10 ng of Aβ(1−40), representing 2.5% of the total coating protein, will attach to each well (*13*). After blocking the excess sites on the plate with 5% bovine serum albumin (BSA), different concentra-

tions of apoA-I (0−115 nM, 100 μL in well) in PBS (pH 7.4) were added to the Aβ(1−40)-coated wells and incubated for 3 h at 37 °C. Bound apoA-I was detected with anti-apoA-I mAb and alkaline phosphatase-conjugated secondary antibody (Jackson Immuno Research Laboratories) and developed with an Attophos substrate kit (Roche, Indianapolis, IN). Nonspecific binding was determined using 5% BSA and omitting Aβ in the assay. The interaction between Aβ(1−40) and 0−570 nM apoE2 and apoE4 (both from Calbiochem) was detected with an anti-apoE mAb (Chemicon, Temecula, CA). Similarly, interactions between Aβ(1−40) and α2M (0−2.3 μM) were detected with an anti-α2M mAb (α2M and anti-α2M mAb from Calbiochem). For inhibition assays, apoA-I was biotinylated with Sulfo-NHS biotin (Pierce) according to the manufacturer's instructions, and free biotin was separated from biotin-labeled apoA-I using Amicon concentration tubes (3 kDa cutoff membranes, Millipore, Bedford, MA). Unlabeled apoA-I, apoE2, and apoE4 (0−2.5 μM), and unlabeled his-APPextra (0−3.9 μM) were coincubated (100 μL) with 25 nM biotin-labeled apoA-I in Aβ(1−40)-coated plates (400 ng per well) for 3 h at 37 °C. Bound biotinylated apoA-I was detected with alkaline phosphatase-labeled streptavidin (Pierce) and evaluated as described above. The data (mean ± SEM) were normalized to the binding of biotin-labeled apoA-I to Aβ without inhibitor and were the result of one experiment performed in quadruplicate. Binding of apoA-I to increasing concentrations of Aβ(1−40) was determined by adding biotin-labeled apoA-I (25 nM) to Aβ(1−40)-coated plates (0.01−10 μM) and detected as above. Nonspecific binding was defined as binding of biotin-labeled apoA-I to Aβ(1−40) in the presence of a 100-fold molar excess of unlabeled apoA-I. Binding and competition data were analyzed using GraphPad Prizm Version 3.0 (San Diego, CA).

Thioflavine T Assay for Aβ(1−40) Aggregation. The thioflavine T assays were performed as previously described (*14*, *15*). Briefly, Aβ(1−40) from Bachem was dissolved at a concentration of 4 mg/mL (1 mM) in dimethyl sulfoxide. The stock was diluted to 0.1 mg/mL (25 μM) of Aβ(1−40) in PBS, filtrated through a 0.22 μm filter, and incubated in a 30 μL volume with different concentrations (0−5 μM) of apoA-I and α2M for 4 days at 37 °C with shaking. As a control, apoA-I (10 μM) was preincubated alone. The incubated samples were added to 50 mM glycine (pH 9.0)/2 μM thioflavine T (Sigma) in a final volume of 2 mL. Fluorescence emission was measured with a Schimadzu spectrofluorophotometer (RF-5301PC) with excitation at 435 nm and emission at 485 nm (bandwidth 10 nm). The data were analyzed by nonlinear regression analysis using GraphPad Prizm Version 3.0.

Congo Red−Aβ Binding. Congo red (CR) binding experiments were performed as described previously (*26*). Briefly, 25 μL of a suspension of Aβ (50 μM) was added to a microtiter plate well containing a 25 μL solution of CR (25 μM) in PBS. After a 30 min incubation at room temperature, the absorbance was read at 541 and 403 nm using a Spectra MAX 340 microplate reader, and the CR-bound Aβ was calculated as follows: $[CR-A\beta]\ (M) = ({}^{541}A_t/47800) - ({}^{403}A_t/68300) - ({}^{403}A_{CR}/86200)$, where ${}^{541}A_t$ equals the absorbance of the CR+Aβ test sample at 541 nm, ${}^{403}A_t$ equals the absorbance of the CR+Aβ test sample at 403 nm, and ${}^{403}A_{CR}$ is the absorbance of the CR-only sample at 403 nm. The data are expressed as the mean ± SEM and are normalized to CR binding to Aβ alone.

Cytotoxicity Assay. The cytotoxic effects of Aβ were assessed by 3-[4,5-dimethylthiazol-2-yl]-2,5-diphenyltetrazolium bromide (MTT) reduction with rat pheochromocytoma PC12 cells as described previously (*27*). Briefly, exponentially growing cells (5000/well) were plated with fresh culture medium (100 μL) on 96-well tissue culture plates and treated 24 h after plating. Aβ dilutions were prepared from a 1 mM stock solution of Aβ in DMEM and either applied fresh or applied after preincubation. For coincubation experiments, apoA-I and α2M were used at 5 and 0.5 μM, respectively. Fibrillar Aβ was obtained by incubating 50 μM peptide in the culture medium either alone or with apoA-I or α2M for 6 days at 37 °C with shaking. Fibril formation was monitored by thioflavine T fluorescence or Congo red binding measurements. After aggregation, Aβ solutions were diluted to 20 μM with fresh medium and added to the cells. The cells were incubated with Aβ for 48 h, and MTT assay was performed as described previously (*27*). Each experiment was performed in triplicate and conducted 3 times with similar results.

RESULTS

Yeast Two-Hybrid Screening. To look for proteins interacting with APPfl, we employed a GAL4-based YTH screen. The APPfl sequence was subcloned into pAS21-1 vector, fusing it to the binding domain (BD) of GAL4 and thus generating pAS2-1APPfl. pAS2-1APPfl was used as bait to screen a YTH liver cDNA library. The YTH screening and β-galactosidase reporter assay studies were performed as previously described (*24*). The expression of BD−APPfl fusion protein was verified by immunoblotting using anti-BD mAb and anti-APP mAb (data not shown). Out of 1×10^6 total clones screened, 300 were β-gal-positive. Using cycloheximide selection, cDNAs for protein partners (fused to the activation domain of GAL4) were isolated. To eliminate false positives, we cotransformed yeast with protein-partner cDNA and pAS2-1APP, or lamin (LAM), or vector alone. Only clones that gave a positive β-gal reaction with APP were considered true positive and were sequenced. Ten of the 98 true positive clones appeared to be apoA-I. They represented two different cDNA clones containing the entire coding region of apoA-I and different parts of the 5′ noncoding region. The interaction between apoA-I and APPfl appeared specific, because apoA-I did not interact with the vector-only construct or the irrelevant lamin protein (Figure 1, panel B).

To identify further domains in APPfl important for the apoA-I interaction, we made two truncated variants of APPfl: one containing the extracellular domain (ectodomain) of APP (APPextra), and the second containing the cytoplasmic tail of APPfl (APPcyto) (Figure 1, panel A). We designed APPextra because apoA-I is a secreted protein and the plaque formation occurs in the extracellular space. To quantify the interaction between apoA-I and APP constructs, we used a liquid *o*-nitrophenyl-β-D-galactosidase colorimetric assay. The results presented in Figure 1B indicate that β-gal activity was significantly greater in yeast clones coexpressing apoA-I and APPfl or APPextra as compared with yeast clones expressing apoA-I and APPcyto. The low β-gal activity seen

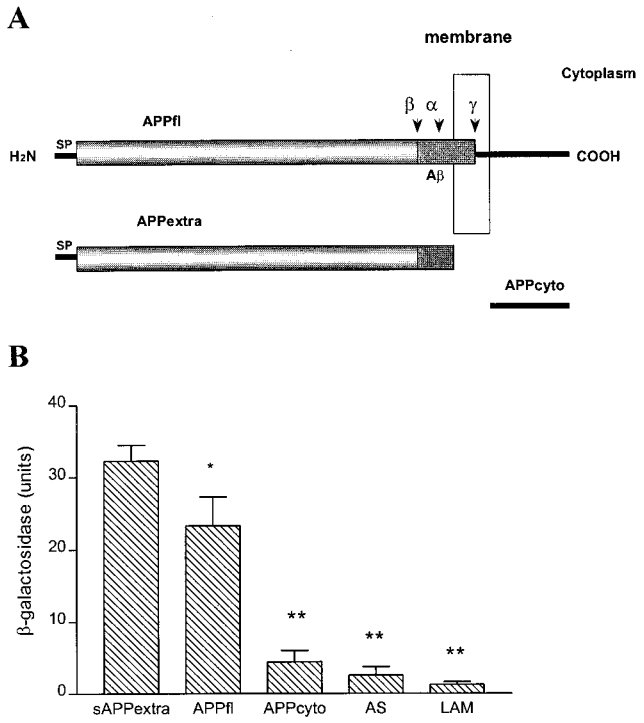

FIGURE 1: ApoA-I and APP interactions in the two-hybrid system. Panel A: APP constructs used in the two-hybrid system. APP constructs were fused to binding domain of GAL4 in pAS2-1 two-hybrid vector. APPfl, full-length APP; APPextra, extracellular domain of APP; APPcyto, cytoplasmic tail of APP; SP, signal peptide. Black area indicates Aβ. The α-, β-, and γ-secretase sites are indicated with arrows. Panel B: Specificity of the apoA-I and APP two-hybrid interaction evaluated by expression of Lac Z reporter gene. β-Galactosidase activity was measured by an *o*-nitrophenyl-β-D-galactosidase colorimetric assay. Yeast were cotransformed with apoA-I in the activation domain vector and various APP constructs in the binding domain vector. Cotransformation of apoA-I with lamin in the binding domain vector (LAM) and vector only (AS) were used as negative controls. Numbers represent the mean ± SEM from five different colony assays measured in triplicate. All results were compared with apoA-I/APPextra transformation. *, $p < 0.05$, **; $p < 0.0001$.

in yeast cotransfected with apoA-I and APPcyto was similar to that with LAM or pAS2-1 (Figure 1, panel B). Thus, the cytoplasmic tail of APPfl did not appear to interact with apoA-I. Interestingly, the β-gal activity in yeast cotransformed with APPextra and apoA-I was significantly higher than that in yeast cotransformed with APPfl and apoA-I ($p < 0.05$), showing that the transmembrane region and cytoplasmic tail of APPfl imposed some conformational hindrance for interaction with apoA-I.

ApoA-I Interacts with APPextra in Vitro. Because of the potentially artificial nature of the YTH system, the extracellular domain of APP may not assume the appropriate structure and thus lead to nonspecific interactions. Therefore, to confirm relevant interactions occurred between APPextra and apoA-I, we attempted to coprecipitate the two proteins. APPextra was expressed as his(6)-tagged protein (his-APPextra), purified, and incubated at various concentrations with apoA-I. The his-APPextra was precipitated from the mixtures with a nickel-affinity resin, and the resulting precipitates were examined for the presence of APPextra by Western blot analysis, using an N-terminal anti-APP monoclonal antibody. As expected, the amount of APPextra precipitated was directly dependent on the APPextra concentration (Figure 2, panel A). The resulting precipitates were also examined for the presence of apoA-I by Western blot analysis, using an anti-apoA-I monoclonal antibody. An apoA-I-immunoreactive protein was clearly observed in the precipitate, and its presence was dependent upon the concentration of APPextra (Figure 2, panel B).

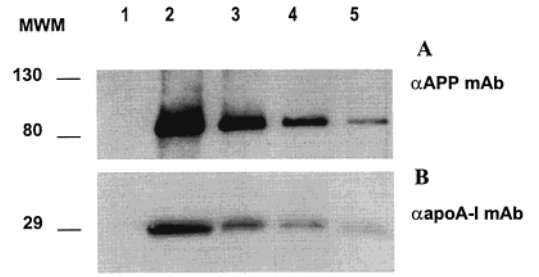

FIGURE 2: ApoA-I and his-APPextra coprecipitation. Panel A: Western blot with N-terminal anti-APP mAb. ApoA-I (300 nM) was incubated for 30 min at 4 °C either alone or with increasing concentrations of his-APPextra. His-APPextra was then affinity-purified with nickel−agarose, and the resulting precipitates were separated on 12% Tris−glycine gels and probed with anti-APP mAb. MWM are molecular weight markers. Panel B: Western blot with anti-apoA-I mAb. ApoA-I and his-APPextra were incubated and precipitated as in panel A, and the blots were probed with anti-apoA-I mAb. His-APPextra concentrations were: lane 1, 0; lane 2, 5 μM; lane 3, 1.25 μM; lane 4, 0.3 μM; and lane 5, 0.08 μM for both panels.

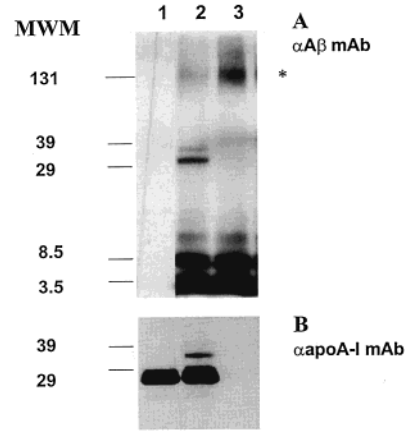

FIGURE 3: SDS-stable complexes with apoA-I and Aβ(1−40). Panel A: Western blot with Aβ1−16 mAb. ApoA-I from human plasma (1 μg) and 4 μg of Aβ(1−40) were incubated at 37 °C for 18 h, and the resultant complexes were separated on 10−20% Tricine gels and probed with anti-Aβ mAb. MWM are molecular weight markers. Panel B: Western blot with anti-apoA-I mAb. The proteins were incubated and resolved as in panel A and probed with anti-apoA-I mAb. Lanes: 1, apoA-I alone; 2, Aβ(1−40) incubated with apoA-I; 3, Aβ(1−40) alone for both panels. The immunoblots are representative of two independent experiments.

ApoA-I Forms SDS-Stable Complexes with Aβ. Because in our YTH and in vitro experiments APPextra contained the extracellular, nontransmembrane portion of Aβ (28 amino acids on the N-terminus of Aβ) (Figure 1, panel A black area), we hypothesized that Aβ may be responsible for the interaction between apoA-I and APP. Therefore, we formally examined if apoA-I associated with Aβ. Synthetic Aβ(1−40) peptide was incubated with apoA-I purified from human plasma. A mixture of apoA-I and Aβ(1−40) in PBS (≈1:17 molar ratio of apoA-I to Aβ) was incubated at 37 °C for 18 h, and resultant complexes were separated on SDS−PAGE. Immunoblotting with anti-Aβ antibody showed Aβ as a

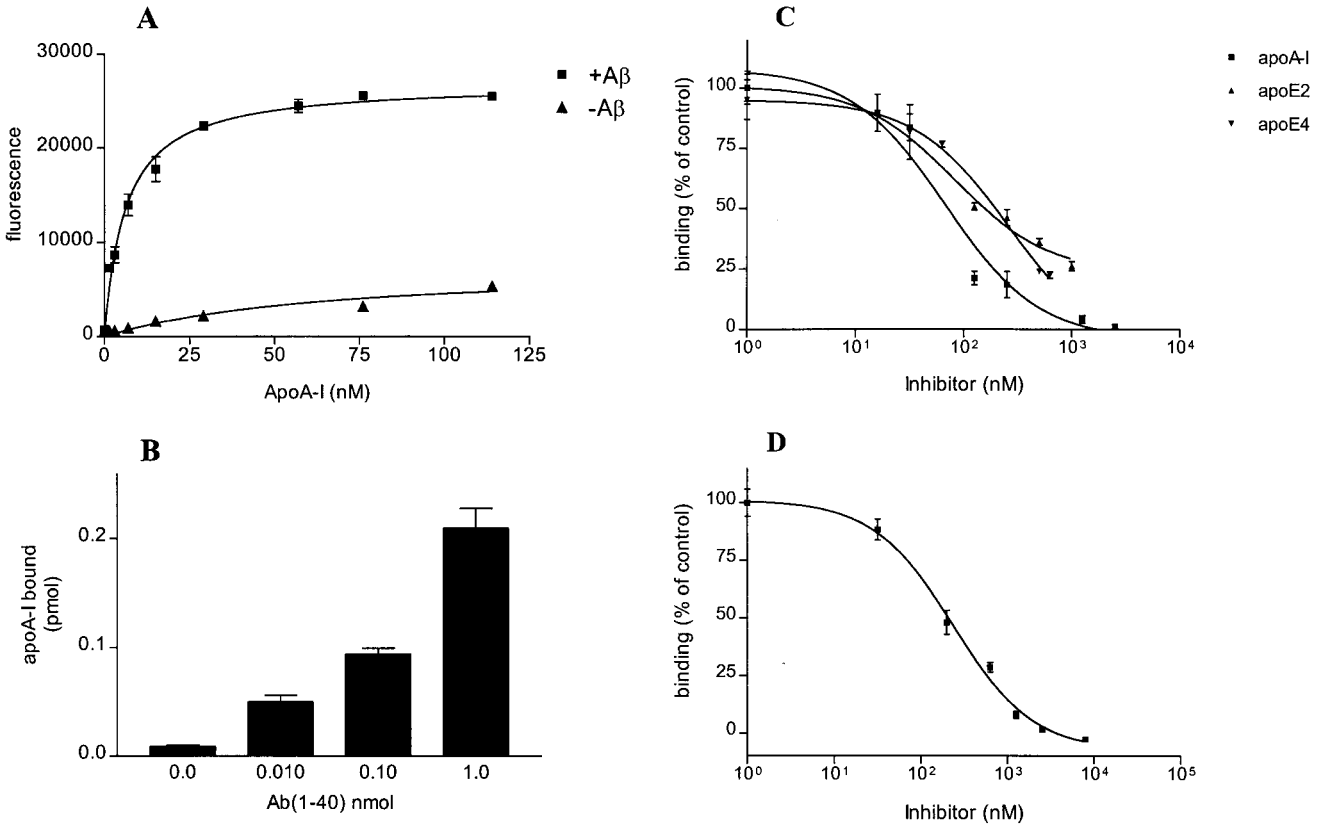

FIGURE 4: Solid-phase ELISA assays. Panel A: Saturation curve for apoA-I−Aβ(1−40) interaction. Variable concentrations (0−115 nM) of apoA-I were incubated with 1 μM Aβ(1−40) (■)- or 5% BSA (▲)-coated wells for 3 h at 37 °C. Bound apoA-I was detected with monoclonal and alkaline phosphatase-labeled anti-mouse antibodies. The means ± SD represent results of three independent experiments, each in triplicate. No bars indicate SD was less than the symbol size. Panel B: Specific binding of biotin-labeled apoA-I to Aβ(1−40) absorbed to microtiter wells. The indicated concentration of Aβ(1−40) was incubated in wells, excess sites on the plate were blocked with 5% BSA, and binding was assayed by adding biotin-labeled apoA-I (25 nM) alone or in the presence of a 100-fold molar excess of unlabeled apoA-I. The mean ± SEM is shown for specific binding: binding of wells incubated with biotin-labeled apoA-I alone (total binding) minus binding in wells incubated with biotin-labeled apoA-I in the presence of 100-fold molar excess of unlabeled apoA-I (nonspecific binding) of quadruplicates. Panel C: Competition experiments. Aβ(1−40) (1 μM) was incubated in wells, and binding was assayed with 25 nM biotin-labeled apoA-I in the presence if increasing amounts of unlabeled apoA-I, apoE2, or apoE4. Biotin-labeled apoA-I was quantitated with alkaline phosphatase-labeled streptavidin. The data (means ± SEM) are result of one experiment in quadruplicate. Panel D: APPextra competition for binding of apoA-I to Aβ(1−40). Aβ(1−40) (1 μM) was incubated in wells, and binding was assayed with 25 nM biotin-labeled apoA-I in the presence of increasing amounts of unlabeled his-APPextra. Biotin-labeled apoA-I was quantified as in panel C. The data (mean ± SEM) are the result of a single experiment performed in quadruplicate.

monomer of approximately 4 kDa, a dimer of 8 kDa, and also higher molecular mass species, probably representing SDS-stable fibrils (Figure 3, panel A, lane 3, marked by asterisk). Lane 1 in Figure 3A demonstrated that the anti-Aβ antibody did not recognize apoA-I alone. When Aβ was incubated with apoA-I, in addition to the Aβ monomer and dimer, we observed an upshifted band of approximately 30−35 kDa, corresponding to the molecular mass of a complexed Aβ−apoA-I (Figure 3, panel A, lane 2). The SDS-stable apoA-I−Aβ monomer complex was also visible after immunoblotting with αapoA-I antibody (Figure 3, panel B, lane 2). With a longer exposure, we detected an apoA-I−Aβ dimer complex (data not shown). We also noticed the high molecular mass SDS-stable Aβ species disappeared after incubation with apoA-I (Figure 3, panel A, lane 2).

Solid-Phase ELISA Assays. To better characterize the interaction of apoA-I−Aβ(1−40), we also used solid-phase ELISA. A concentration−response relationship that reached saturation was obtained when increasing concentrations of unlabeled apoA-I were allowed to interact with a constant amount of immobilized Aβ(1−40) (Figure 4, panel A). Minimal nonspecific binding was seen. Using nonlinear regression analysis of the specific binding data fitted to a rectangular hyperbola, we calculated the dissociation constant (K_d) as 6 nM. As a control, we used α2M and apoE isoforms (apoE2 and apoE4) that were shown previously to bind Aβ-(1−40) with high affinity (*14*). α2M was applied at concentrations ranging from 0 to 2.3 μM, and the calculated K_d was 304 nM, corresponding to a previously reported value (*14*). Using the same binding conditions, we calculated a K_d for apoE2 and apoE4 of 15 and 19 nM, respectively. Therefore, apoA-I showed the highest affinity toward Aβ-(1−40) among the binding partners of Aβ that were used.

To determine the specificity of the apoA-I and Aβ(1−40) interaction, we incubated biotin-labeled apoA-I in microtiter wells coated with increasing concentrations of Aβ(1−40). As visible from Figure 4B, biotin-labeled apoA-I bound to Aβ(1−40)-coated microtiter wells in a manner that was dependent on the concentration of Aβ(1−40). In separate experiments, the reversibility of the interaction was assessed using biotin-labeled apoA-I at a concentration of 25 nM. The binding of biotin-labeled apoA-I to immobilized Aβ(1−40) was competitively inhibited by increasing concentrations of unlabeled apoA-I (Figure 4, panel C). The data fitted a one-

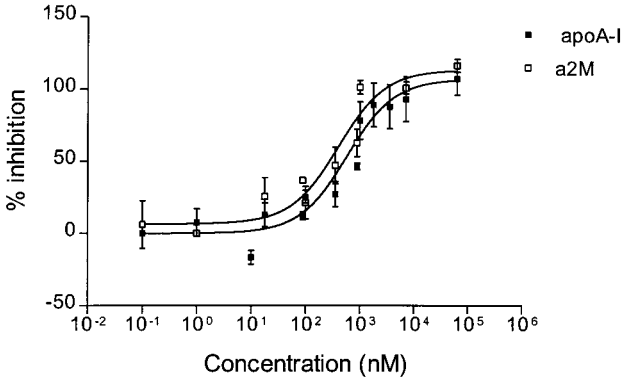

FIGURE 5: Thioflavine T assay for monitoring Aβ1−40 aggregation. 25 μM Aβ(1−40) was incubated at 37 °C for 4 days in PBS with apoA-I or α2M, each at a range of concentrations (0−10^6 nM). IC_{50} for apoA-I−Aβ(1−40) interaction was 582 ± 7.3 nM, and IC_{50} for α2M−Aβ(1−40) interaction was 400 ± 5.3 nM. Values represent means ± SEM, $n = 6$.

site competition curve with a half-maximal inhibition (IC_{50}) of 66 nM. We also performed competitive inhibition experiments using apoE2 and apoE4. Increasing concentrations of apoE2 and apoE4 competitively inhibited the binding of biotin-labeled apoA-I to Aβ(1−40) with an IC_{50} for apoE2 and apoE4 of 125 and 261 nM, respectively (Figure 4, panel C), indicating that apoA-I had the highest affinity for Aβ-(1−40). To determine if APPextra could compete for binding of apoA-I to Aβ(1−40), we incubated increasing concentrations of his-APPextra with biotin-labeled apoA-I in Aβ(1−40)-coated microtiter wells. As visible from Figure 4D, APPextra completely inhibited the binding of biotin-labeled apoA-I with an IC_{50} of 235 nM. Therefore, we concluded that APPextra can block the interaction between apoA-I and Aβ(1−40), probably because of the presence of the Aβ domain.

Effect of ApoA-I on in Vitro Fibril Formation. Previously it has been suggested that apoA-I as well as apoE act as pathological chaperones targeting Aβ for amyloid deposits (*19*). The disappearance of high molecular weight aggregates of Aβ observed when Aβ was coincubated with apoA-I (Figure 3, Panel A) prompted us to investigate whether apoA-I had effects on Aβ in vitro fibril formation. Thus, we used thioflavine T that interacts with crossed β-sheet structures common to the aggregated amyloid proteins (*28*). Aβ was incubated with different concentrations of apoA-I (0−5 μM). As visible from Figure 5 apoA-I significantly inhibited Aβ(1−40) aggregation with an IC_{50} of 580 nM. In this assay, we found α2M inhibited Aβ aggregation with an IC_{50} of 400 nM, confirming previous studies (*14*). Therefore, apoA-I had an antiaggregation effect on Aβ(1−40) fibril formation with an IC_{50} that approximated the IC_{50} of α2M.

Effect of ApoA-I on Aβ-Induced Toxicity. Because previous work has demonstrated that both fibrillar and nonfibrillar forms of Aβ(1−40) are neurotoxic, we investigated whether apoA-I was also able to attenuate Aβ(1−40)-induced toxicity. We used rat pheochromocytoma PC12 cells to study the cytotoxic effect of Aβ in the presence or absence of apoA-I or α2M. The effects of apoA-I and α2M on Aβ-induced toxicity were assessed with the widely used measurements of MTT reduction. As visible from Figure 6A, both apoA-I and α2M decreased the cytotoxicity of freshly prepared, nonfibrillar Aβ. Similarly, apoA-I attenuated Aβ-induced cytotoxicity when preincubated with Aβ for 6 days (Figure 6B). Correspondingly, CR binding experiments showed that concomitant incubation of apoA-I with Aβ for 6 days decreased Aβ fibril formation approximately 90% (Figure 6C). The protective effect of apoA-I on Aβ fibril formation was comparable to that seen with α2M.

DISCUSSION

ApoA-I is a 243 amino acid polypeptide and the major protein moiety of HDL. The gene encoding apoA-I is a member of the apolipoprotein multigene superfamily, which includes genes encoding exchangeable apolipoproteins (apoA-I, A-II, and E). They are thought to have evolved from a common ancestor by duplication/deletion of a 33 amino acid motif. ApoA-I contains 22- or 11-residue repeat units, folding into 6−8 putative amphipatic α-helixes, which allow the interaction of the protein with lipids through its hydrophobic face (*29*). There is an inverse relationship between HDL plasma levels and coronary heart disease that has been attributed to the role HDL and apoA-I play in the reverse cholesterol transport. The efficiency of reverse cholesterol transport depends on the specific ability of apoA-I to promote cellular cholesterol efflux, bind lipids, activate lecithin: cholesterol acyltransferase, and form mature HDL (*30*). While the expression and the function of apoA-I in the peripheral tissues are well established, little is known about its origin and role in the central and peripheral nervous system (*22*, *29*). ApoA-I mRNA and synthesis have been detected in the microvascular endothelial cells in the brain (*31*), but there is no evidence for apoA-I synthesis in other cells of the central nervous system (*32*). Therefore, we cannot exclude the possibility that our observations have relevance only to peripheral tissues. Nonetheless, the normal level of apoA-I in plasma is 1.5 g/L, and in CSF it is presented at 0.4% of its plasma concentration (*22*, *33*). Although there is no direct evidence that apoA-I and apoE regulate cholesterol homeostasis in the central nervous system as they do in peripheral cells, it is interesting that lecithin:cholesterol acyltransferase is expressed in the brain and apoA-I can activate it, providing a mechanism for transporting brain cholesterol. Marked increases in apoA-I concentrations in CSF were observed in poliovirus-infected macaques and in patients with acute meningitis, suggesting that apoA-I may be involved in the mobilization and redistribution of lipids in repair of myelin and axonal membranes after injury or infection (*34*, *35*). The serum concentration of apoA-I is significantly decreased in AD patients as compared with the normal population, but the CSF level is unchanged (*36*−*38*). Recently Fagan et al. found that the levels of apoA-I and cholesterol in CSF lipoproteins of healthy, cognitively normal individuals are correlated with levels in plasma, suggesting a role for plasma apoA-I in central nervous system lipoprotein metabolism (*46*). The possibility of a genetic association between AD and alleles at the apoA-I/CIII loci has been examined, but no obvious genetic link to these loci was found (*39*).

Many of the brain apolipoproteins, like apoA-I, apoE, and apoJ, have been found in the SP and Aβ deposits in cerebral blood vessels (*20*, *40*). Aβ was also reported to coimmunoprecipitate with apolipoproteins from CSF, to interact with normal serum HDL, and to bind in vitro a number of apolipoproteins (*19*, *21*, *41*, *42*). This suggests that exchange-

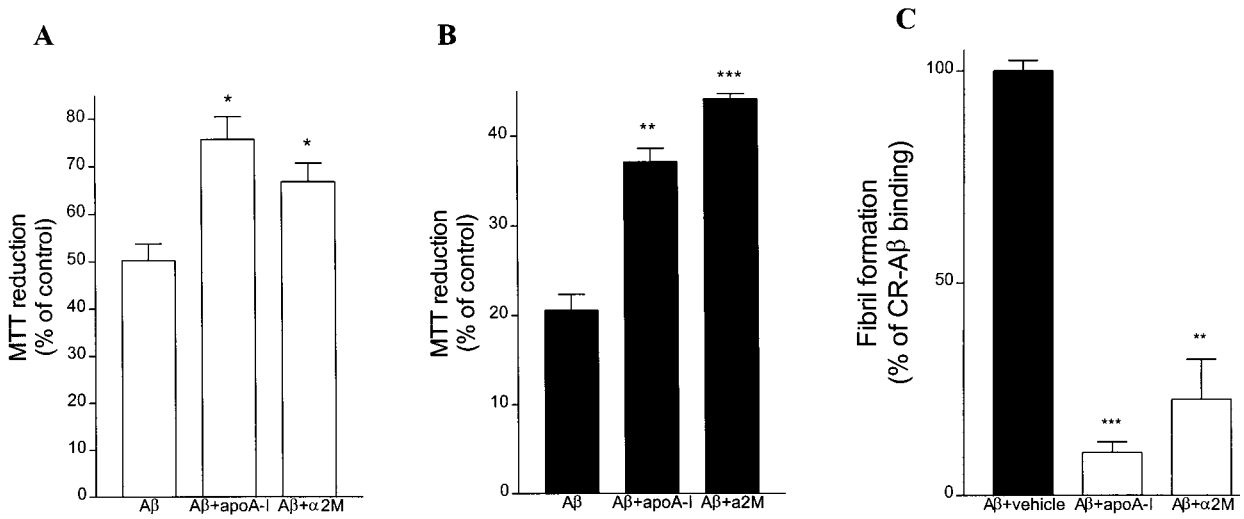

FIGURE 6: Effect of apoA-I and α2M on the toxicity induced by nonfibrillar and fibrillar Aβ. PC12 cells were incubated with 10 μM nonfibrillar Aβ (A) or 20 μM fibrillar Aβ (B) in the absence or presence of apoA-I (5 μM) or α2M (0.5 μM). Fibrillar Aβ was obtained as described under Materials and Methods. Aβ-induced toxicity was evaluated using the MTT assay. Each experiment was performed in triplicate. The data are expressed as the mean ± SEM and are normalized to the vehicle control. (C) ApoA-I and α2M prevented Aβ aggregation. Aβ (50 μM) was preincubated with apoA-I (5 μM) or α2M (0.5 μM) for 6 days, and Aβ fibril formation was measured by CR binding. The data are expressed as the mean ± SEM, $n = 3$, and are normalized to CR binding to Aβ alone (CR−Aβ binding). *, $p < 0.05$; **, $p < 0.01$; ***, $p < 0.001$ compared to Aβ alone by Student's t test.

able apolipoproteins including apoA-I and apoE may be carrier proteins for Aβ in plasma and CSF through their common amphipatic α-helices facilitating its clearance. It is worth noting that apolipoproteins and Aβ may interact nonspecifically, because of their hydrophobic nature. Nevertheless, the data presented here demonstrate that apoA-I−Aβ interaction was saturable, specific, and reversible. Moreover, apoA-I bound Aβ in vitro with 2−3 times greater affinity than apoE2 and apoE4. The competition experiments performed with apoE2 and apoE4 showed that they were less efficient than apoA-I itself in inhibiting apoA-I−Aβ complex formation, apoE4 having 4 times higher IC_{50} than apoA-I. ApoE levels, however, are considerably greater than apoA-I levels, which is not synthesized in the brain. In our study, we have demonstrated for the first time that apoA-I decreased Aβ aggregation with an IC_{50} comparable to that of α2M, which is a well-known inhibitor of Aβ fibril formation. Accordingly, we were able to show that apoA-I attenuated Aβ-induced cellular toxicity.

We have also found that apoA-I interacted with APPfl and APPextra in YTH assay. Because the YTH system may be too artificial, our complementary studies with APPextra in vitro were important. It should be noted, however, that no lipids were added to our assays and this might influence any interactions in vitro. The overall structure of APP suggests it might function as a receptor or growth factor (*4*), and several functional domains in APPextra have been identified. For example, the RERMS sequence (amino acids residues 328−332 of APP_{695}) seems to have growth-promoting properties (*43*) or to stimulate mitogenesis (*12*). There are also heparin, Cu(II), and Zn(II) binding domains (*44*, *45*). The carboxy-terminal 16 amino acids of sAPPα, that distinguish the 2 alternative sAPPs resulting from α- and β-secretase processing, have been shown to protect hippocampal neurons from damage induced by ischemia, glucose deprivation, and glutamate (*12*). Therefore, binding of apoA-I to APPextra might modulate any of the above-mentioned effects. Our future efforts should be to determine which sequences in APPextra are essential for the binding with apoA-I.

ACKNOWLEDGMENT

We are grateful to Marc DiSabella and John Skoko for the excellent technical help in cloning and protein purification experiments.

REFERENCES

1. Selkoe, D. J. (1997) *Science 275*, 630−631.
2. West, M. J., Coleman, P. D., Flood, D. G., and Troncoso, J. C. (1994) *Lancet 344*, 769−772.
3. Dickson, D. W., and Yen, S. H. (1989) *Neurobiol. Aging 10*, 402−404.
4. Kang, J., Lemaire, H. G., Unterbeck, A., Salbaum, J. M., Masters, C. L., Grzeschik, K. H., Multhaup, G., Beyreuther, K., and Muller-Hill, B. (1987) *Nature 325*, 733−736.
5. Tanzi, R. E., Gusella, J. F., Watkins, P. C., Bruns, G. A., St. George-Hyslop, P., Van Keuren, M. L., Patterson, D., Pagan, S., Kurnit, D. M., and Neve, R. L. (1987) *Science 235*, 880−884.
6. Williamson, T. G., Mok, S. S., Henry, A., Cappai, R., Lander, A. D., Nurcombe, V., Beyreuther, K., Masters, C. L., and Small, D. H. (1996) *J. Biol. Chem. 271*, 31215−31221.
7. Vassar, R., Bennett, B. D., Babu-Khan, S., Kahn, S., Mendiaz, E. A., Denis, P., Teplow, D. B., Ross, S., Amarante, P., Loeloff, R., Luo, Y., Fisher, S., Fuller, J., Edenson, S., Lile, J., Jarosinski, M. A., Biere, A. L., Curran, E., Burgess, T., Louis, J. C., Collins, F., Treanor, J., Rogers, G., and Citron, M. (1999) *Science 286*, 735−741.
8. Selkoe, D. J., and Wolfe, M. S. (2000) *Proc. Natl. Acad. Sci. U.S.A. 97*, 5690−5692.
9. Lammich, S., Kojro, E., Postina, R., Gilbert, S., Pfeiffer, R., Jasionowski, M., Haass, C., and Fahrenholz, F. (1999) *Proc. Natl. Acad. Sci. U.S.A. 96*, 3922−3927.
10. Buxbaum, J. D., Liu, K. N., Luo, Y., Slack, J. L., Stocking, K. L., Peschon, J. J., Johnson, R. S., Castner, B. J., Cerretti, D. P., and Black, R. A. (1998) *J. Biol. Chem. 273*, 27765−27767.
11. Mattson, M. P., Cheng, B., Culwell, A. R., Esch, F. S., Lieberburg, I., and Rydel, R. E. (1993) *Neuron 10*, 243−254.
12. Barger, S. W., and Mattson, M. P. (1997) *J. Neurochem. 69*, 60−67.

13. Matsubara, E., Frangione, B., and Ghiso, J. (1995) *J. Biol. Chem. 270*, 7563−7567.
14. Hughes, S. R., Khorkova, O., Goyal, S., Knaeblein, J., Heroux, J., Riedel, N. G., and Sahasrabudhe, S. (1998) *Proc. Natl. Acad. Sci. U.S.A. 95*, 3275−3280.
15. Castano, E. M., Prelli, F., Wisniewski, T., Golabek, A., Kumar, R. A., Soto, C., and Frangione, B. (1995) *Biochem. J. 306*, 599−604.
16. Monji, A., Yoshida, I., Tashiro, K., Hayashi, Y., Matsuda, K., and Tashiro, N. (2000) *Neurosci. Lett. 278*, 81−84.
17. Corder, E. H., Saunders, A. M., Strittmatter, W. J., Schmechel, D. E., Gaskell, P. C., Small, G. W., Roses, A. D., Haines, J. L., and Pericak-Vance, M. A. (1993) *Science 261*, 921−923.
18. Aleshkov, S., Abraham, C. R., and Zannis, V. I. (1997) *Biochemistry 36*, 10571−10580.
19. Golabek, A., Marques, M. A., Lalowski, M., and Wisniewski, T. (1995) *Neurosci. Lett. 191*, 79−82.
20. Harr, S. D., Uint, L., Hollister, R., Hyman, B. T., and Mendez, A. J. (1996) *J. Neurochem. 66*, 2429−2435.
21. Koudinov, A. R., Berezov, T. T., Kumar, A., and Koudinova, N. V. (1998) *Clin. Chim. Acta 270*, 75−84.
22. Wood, W. G., Schroeder, F., Avdulov, N. A., Chochina, S. V., and Igbavboa, U. (1999) *Lipids 34*, 225−234.
23. Lefterov, I. M., Koldamova, R. P., and Lazo, J. S. (2000) *FASEB J. 14*, 1837−1847.
24. Koldamova, R. P., Lefterov, I. M., Gadjeva, V. G., and Lazo, J. S. (1998) *Biochemistry 37*, 2282−2290.
25. Koldamova, R. P., Lefterov, I. M., DiSabella, M. T., and Lazo, J. S. (1998) *Mol. Pharmacol. 54*, 954−961.
26. Klunk, W. E., Jacob, R. F., and Mason, R. P. (1999) *Methods Enzymol. 309*, 285−305.
27. Shearman, M. S. (1999) *Methods Enzymol. 309*, 716−723.
28. LeVine, H. (1999) *Methods Enzymol. 309*, 274−284
29. Stoffel, W. (1984) *J. Lipid Res. 25*, 1586−1592.
30. Yokoyama, S. (1998) *Biochim. Biophys. Acta 1392*, 1−15.
31. Weiler-Guttler, H., Sommerfeldt, M., Papandrikopoulou, A., Mischek, U., Bonitz, D., Frey, A., Grupe, M., Scheerer, J., and Gassen, H. G. (1990) *J. Neurochem. 54*, 444−450.
32. Fujita, S. C., Sakuta, K., Tsuchiya, R., and Hamanaka, H. (1999) *Neurosci. Res. 35*, 123−133.
33. Roheim, P. S., Carey, M., Forte, T., and Vega, G. L. (1979) *Proc. Natl. Acad. Sci. U.S.A. 76*, 4646−4649.
34. Song, H., Seishima, M., Saito, K., Maeda, S., Takemura, M., Noma, A., Kondo, A., Manabe, M., Urakami, K., and Nakashima, K. (1998) *Ann. Clin. Biochem. 35*, 408−414.
35. Saito, K., Seishima, M., Heyes, M. P., Song, H., Fujigaki, S., Maeda, S., Vickers, J. H., and Noma, A. (1997) *Biochem. J. 321*, 145−149.
36. Merched, A., Xia, Y., Visvikis, S., Serot, J. M., and Siest, G. (2000) *Neurobiol. Aging 21*, 27−30.
37. Song, H., Saito, K., Seishima, M., Noma, A., Urakami, K., and Nakashima, K. (1997) *Neurosci. Lett. 231*, 175−178.
38. Fukuyama, R., Mizuno, T., Mori, S., Yanagisawa, K., Nakajima, K., and Fushiki, S. (2000) *Eur. Neurol. 43*, 161−169.
39. Houlden, H., Crook, R., Duff, K., Hutton, M., Collinge, J., Roques, P., Rossor, M., and Hardy, J. (1995) *Neurosci. Lett. 188*, 202−204.
40. Wisniewski, T., Golabek, A. A., Kida, E., Wisniewski, K. E., and Frangione, B. (1995) *Am. J. Pathol. 147*, 238−244.
41. LaDu, M. J., Falduto, M. T., Manelli, A. M., Reardon, C. A., Getz, G. S., and Frail, D. E. (1994) *J. Biol. Chem. 269*, 23403−23406.
42. Jarrett, J. T., Berger, E. P., and Lansbury, P. T. J. (1993) *Biochemistry 32*, 4693−4697.
43. Ninomiya, H., Roch, J. M., Sundsmo, M. P., Otero, D. A., and Saitoh, T. (1993) *J. Cell Biol. 121*, 879−886.
44. Bush, A. I., Multhaup, G., Moir, R. D., Williamson, T. G., Small, D. H., Rumble, B., Pollwein, P., Beyreuther, K., and Masters, C. L. (1993) *J. Biol. Chem. 268*, 16109−16112.
45. White, A. R., Multhaup, G., Maher, F., Bellingham, S., Camakaris, J., Zheng, H., Bush, A. I., Beyreuther, K., Masters, C. L., and Cappai, R. (1999) *J. Neurosci. 19*, 9170−9179.
46. Fagan, A. M., Younkin, L. H., Morris, J. C., Fryer, J. D., Cole, T. G., Younkin, S. G., Holtzman, D. M. (2000) *Ann. Neurol. 48*, 201−210.

BI002186K